Injection and Trapping of Tunnel-Ionized Electrons into Laser-Produced Wakes

A. Pak,[1] K. A. Marsh,[1] S. F. Martins,[3,2] W. Lu,[2] W. B. Mori,[2] and C. Joshi[1]

[1]*Department of Electrical Engineering, UCLA, Los Angeles, California 90095, USA*
[2]*Department of Physics and Astronomy, UCLA, Los Angeles, California 90095, USA*
[3]*GoLP/Instituto de Plasmas e Fusão Nuclear, Instituto Superior Técnico, Lisbon, Portugal*

(Received 3 August 2009; published 15 January 2010)

A method, which utilizes the large difference in ionization potentials between successive ionization states of trace atoms, for injecting electrons into a laser-driven wakefield is presented. Here a mixture of helium and trace amounts of nitrogen gas was used. Electrons from the K shell of nitrogen were tunnel ionized near the peak of the laser pulse and were injected into and trapped by the wake created by electrons from majority helium atoms and the L shell of nitrogen. The spectrum of the accelerated electrons, the threshold intensity at which trapping occurs, the forward transmitted laser spectrum, and the beam divergence are all consistent with this injection process. The experimental measurements are supported by theory and 3D OSIRIS simulations.

DOI: 10.1103/PhysRevLett.104.025003 PACS numbers: 52.38.Kd, 41.75.Jv, 52.35.Mw

Acceleration of electrons using laser-driven plasma wakes is an active area of research. The longitudinal electric field of such wakes has been used to accelerate plasma electrons to energies up to 1 GeV in a few centimeters [1]. Currently, significant effort is being directed towards developing new methods of injecting electrons into a laser wakefield accelerator (LWFA) for improving the reliability and efficiency of this scheme [2–6]. Controlling the injection process could be used to vary the charge, divergence, and energy of the accelerated electrons. Recent work in both electron and laser-driven wakefields has indicated that in a partially ionized plasma, electrons can be injected into the wake due to ionization by the electron or the laser field [7,8]. Here we extend this idea to the LWFA operating in the self-guided blowout regime, where the field of the laser is used to control the injection process into the wakefield. This additional degree of freedom will permit the trapping of electrons at lower plasma densities, using lower laser intensities than are currently required for the self-trapping of plasma electrons that form the wake. This technique has the potential to generate GeV class electron beams with low beam divergences and will allow studies of energy extraction efficiency by beam-loading of such wakes.

Figure 1 illustrates the principles of the tunneling ionization injection and trapping of electrons into a LWFA using the code OSIRIS [9]. The wakefield is excited in a plasma created from a gas or a gas mixture that has multiple ionization states. Experiments reported here were carried out in a mixture of helium and trace amounts of nitrogen gas, although it may be desirable to use other trace atoms with multiple ionization states depending on the plasma density and laser conditions that are used. The leading edge of the ultrashort laser pulse is intense enough to fully ionize helium atoms and the outer five electrons of nitrogen. The ponderomotive force of the laser pushes out these electrons, creating a wake. There is a large difference between the ionization potential (IP) and thus the ionization appearance intensity of the 5th (L-shell) electron that produces N^{5+} (IP 98 eV) and the two K-shell electrons that produce N^{6+} and N^{7+} (IP 552 and 667 eV, respectively).

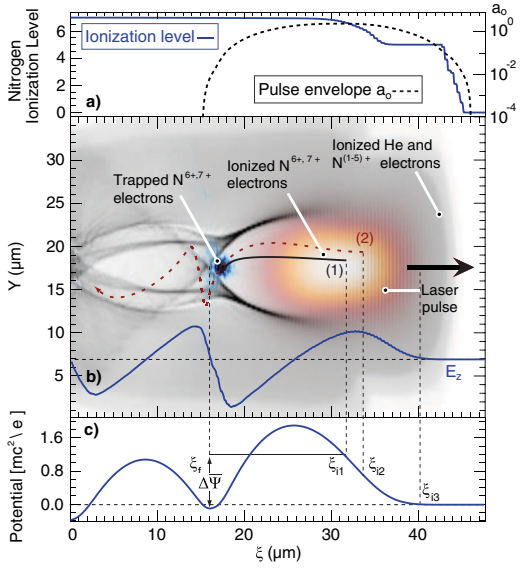

FIG. 1 (color online). OSIRIS simulation of the injection of tunnel-ionized electrons ($n_e = 7 \times 10^{18}$ cm^{-3}; $a_0 = 2$). As the laser pulse propagates to the right it ionizes a 9:1 mix of He and N_2 and drives a wake. (a) The envelope of the normalized vector potential a_o of the laser (dashed line) and the ionization state of nitrogen atoms (solid line) on axis. The superimposed trajectories (1) and (2) in frame (b) represent simulation electrons ionized into the wake from the K shell of nitrogen. Electron (1) is ionized close to the axis and is trapped by the wakefield, while electron (2), ionized earlier and off axis, slips over the potential well and is not trapped. The solid line labeled E_z refers on axis longitudinal electric field of the wake. (c) The normalized wake potential $\bar{\Psi}$ on axis, with particular points relevant to the physics of the trapping mechanism depicted.

This step in the ionization potential can be matched to the laser intensity profile and the plasma density, such that the 6th and 7th nitrogen electrons are tunnel ionized by the electric field of the laser and injected into the electric field of the fully formed wake, as shown in Fig. 1. These ionized electrons appear at rest and slip backwards relative to the laser pulse and the wake. If they gain enough energy from the longitudinal electric field (E_z) of the first period of the wake to move at the phase velocity of the wake v_ϕ, they are trapped and will gain additional energy as they now move forward with respect to the wake.

Experiments were conducted at UCLA using a Ti:sapphire laser with laser pulse energies $\leq$500 mJ and an average pulse width of ~45 fs (FWHM). The laser pulse was focused to a spot size of 6 μm onto the edge of a 2 mm wide column of gas created by a conical gas jet. The normalized vector potential a_o of the laser pulse in these experiments ranged from 1.6 to 2.5. Interferometric measurements using a ~70 fs probe beam indicate that the typical plasma electron density profile (not shown) consisted of a 700 μm density up-ramp followed by a 500 μm plateau at a density $n_e \sim 1.4 \times 10^{19}$ cm^{-3} and then a 700 μm density down ramp. Generated electron beams were dispersed in the plane of laser polarization onto a LANEX screen, placed 16 cm from a dipole magnet with a magnetic field ~1 T extending over 6.5 cm.

The formation of a preplasma can defocus the laser and reduce the coupling of laser power to the wake. The IP of the outermost nitrogen electron (14.5 eV) is lower than that of the first helium electron (24.5 eV). This makes a pure nitrogen gas more susceptible to ionization from a laser prepulse than a pure helium gas. Therefore in this work a mixture of 90% helium and 10% nitrogen gas (He:N_2) was used to reduce these effects.

The measured electron spectra obtained at a laser a_o of 2.35 and 1.64 are shown in Figs. 2(a) and 2(b), respectively. The broad electron spectrum observed in Fig. 2(a) is consistent with the continuous injection and acceleration of electrons from the K-shell of nitrogen. Lowering the laser intensity [Fig. 2(b)] can limit the distance over which the laser pulse is intense enough to ionize the 6th nitrogen

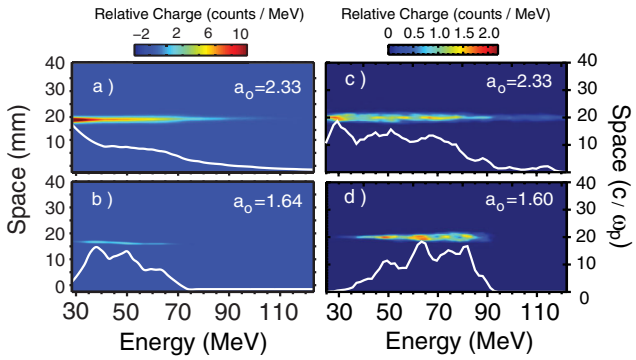

FIG. 2 (color online). A comparison between the observed (a) and (b) and the simulated (c) and (d) electron spectra created at a $n_e \sim 1.4 \times 10^{19}$ cm^{-3} from a 9:1 He:N_2 gas mix.

electron into the wake. When the injection of electrons is stopped, the wake will continue to accelerate previously trapped electrons. If a significant amount of acceleration takes place after the injection of electrons has stopped, then there will be an absence of a low energy tail in the observed spectrum as seen in Fig. 2(b). In future experiments, a two cell arrangement, where the first cell contains a mixture of two species for injection (He:N_2 for example) and a second accelerator stage containing only one gas (e.g. He) would allow for narrower energy spread beams to be obtained.

Electron spectra shown in Figs. 2(c) and 2(d) are generated using 3D OSIRIS particle-in-cell code simulations [9] which included ionization effects using the ADK model [10]. In these simulations, the laser energy, spot size, pulse width, as well as the gas mixture ratio and plasma density profile were the same as the experimental values stated above. By tracking the ionization state in the simulations, it was found that the two helium and the outer five electrons of nitrogen only formed the wake and were not trapped. The simulated spectra shown in Fig. 2(c) and 2(d) are comprised only from electrons from the K shell of nitrogen. This confirms that it is indeed electrons from the K shell that are injected and accelerated preferentially due to being ionized into the wakefield.

The simulated spectra at both laser intensities are in qualitative agreement with the spectra observed in the experiment. In both the experiment and simulations, the energy spread of the accelerated electrons is found to decrease as a_o is decreased, from being continuous at a_o of 2.33 to $\Delta E/E \simeq .6$ at an a_o of 1.6. With $n_e = 1.4 \times 10^{19}$ cm^{-3} and $a_o = 2.3$, the maximum energy gain given by the 3D nonlinear theory [11], $E(\mathrm{MeV}) \approx (1/3) \times (\omega_o/\omega_p)^2 a_o$, is 92 MeV, which is close to the observed value. Here ω_o and ω_p are the laser and plasma frequency, respectively. Simulations indicate that the continuous electron ionization and injection leads to a decrease in the potential of the wake. This can eventually limit amount of charge trapped as well as the final energy accelerated electrons reach.

The intensity threshold for this trapping process was measured by varying the a_o of the laser at a fixed plasma density. Figure 3 is a plot of the relative total charge, with energies above 25 MeV, of the dispersed electron beam versus initial a_o. The shaded region of Fig. 3 indicates that electron spectra were not observed below an a_o of 1.6. This sharp intensity threshold, which is slightly below the a_o required to ionize the 6th electron from nitrogen, suggests that the trapped and accelerated electrons are indeed from the K shell of nitrogen. At the threshold for observed accelerated charge, the power of the laser pulse was ~1.4 times the critical power for self-focusing (P_c) [12]. Therefore it is likely (and it is observed in present simulations) that the intensity of the laser pulse increased as the initial spot size of 6 μm is focused by the plasma to the matched blowout radius of ~4 μm [13]. This process allows the laser to ionize and inject the 6th electron of

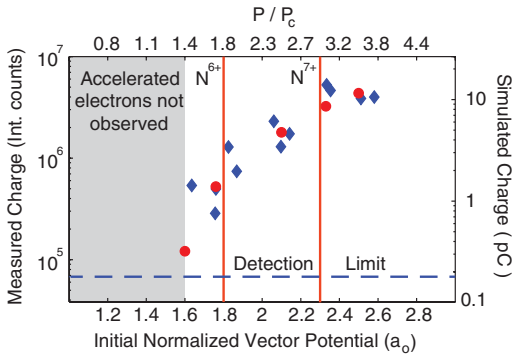

FIG. 3 (color online). Measured (diamonds) and simulated (circles) integrated charge of electrons with energy >25 MeV vs laser a_o and normalized power P/P_c. Solid lines correspond to the a_o required to ionize the 6th and 7th electron of nitrogen in one cycle of the laser pulse using the ADK model. Dashed line is the experimental signal detection limit. $n_e \sim 1.4 \times 10^{19}$ cm^{-3}; 9:1 He:N_2 gas mix.

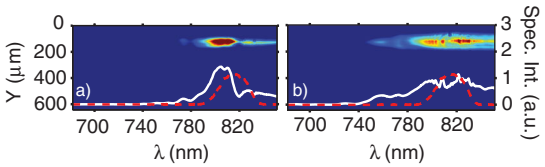

FIG. 4 (color online). The measured spectral intensity of the laser pulse (solid line) observed after propagating through a plasma created from pure helium gas (a) and from a 9:1 He:N_2 gas mix (b). For both spectra n_e was $\sim 1.5 \times 10^{19}$ cm^{-3} and $a_o \approx 1.65$. The dashed line is the normalized spectral intensity of the laser.

nitrogen, even when the initial a_o is below the corresponding ionization threshold. The increase in total charge with a_o is thought to be due to the larger volume of ionized and injected electrons that occurs at higher laser intensities. Figure 3 indicates that the trapping threshold and the relative trend in total accelerated charge seen in the experiment are in good agreement with those seen in the simulations. Simulations indicate that the evolution of the laser pulse is not critical to the injection and trapping of electrons once the laser intensity rises above the ionization appearance intensity for $N^{6+,7+}$. As a comparison, in the blowout regime, previous simulations have indicated that self-trapping of electrons into the first period of the wake requires an a_o of 4.3 [14]. A recent overview of many experiments [15] has found that an a_o of ~3.8 was required to self-trap wake electrons consistently. These vector potentials are larger than the threshold value of a_o seen for ionization trapping of the 6th nitrogen electron here.

Figure 4 shows the spectrum of the laser pulse measured after propagating through a plasma created from pure helium gas and the He:N_2 gas mix close to the threshold intensity to produce N^{6+}. Transmitted spectra contain frequencies not present in the vacuum laser spectrum. Locally the frequency of the laser pulse can be increased and decreased by the wake via photon acceleration and deceleration [16]. Additionally, ionization of the gas causes an increase in the local electron density which further blueshifts the laser frequencies [17]. The spectra were measured by image relaying the exit plane of the plasma onto the slit of an imaging spectrograph. The self-guided portion of the transmitted spectrum shown in Fig. 4 was much brighter than the unguided spectrally blue shifted laser light associated with the initial ionization process that forms the plasma (not seen here). Experimental constraints did not allow for the simultaneous use of a LANEX screen and spectrograph. Therefore, a surface barrier detector (SBD) was used to indirectly detect the presence of electrons by monitoring the x-ray bremsstrahlung radiation created from collisions between accelerated electrons and components within the vacuum chamber.

If the laser pulse remains well guided as it ionizes and injects electrons into the wake, then the guided portion of the transmitted spectrum from the He:N_2 gas mix is expected to show a greater blue shift than in pure helium. This is indeed observed in our experiments. A strong SBD signal was observed in conjunction with the extended blue shifted spectrum of the transmitted laser pulse from the He:N_2 mix shown in Fig. 4(b). Below an a_o of 1.6 this additional blue shift in the transmitted laser light in the He:N_2 plasma is not observed.

The divergence for accelerated electron beams is expected to be low near the injection threshold, as electrons are predominantly ionized on axis near the peak laser intensity and do not undergo large betatron oscillations [18]. However, as a consequence of being ionized within the field of the laser, trapped electrons will gain an additional amount of momentum with a component in the direction of the laser field polarization [6,19]. This effect leads to a beam with an asymmetrical divergence (3 vs 6.3 mrad) as shown in the inset of Fig. 5. Additionally, Fig. 5 indicates that the divergence transverse to the laser polarization initially remains relatively constant for $a_o < 2.3$, but subsequently increases as the laser a_o is increased. A possible explanation for this trend, which is also seen in simulations, is that as a_o is raised, electrons are ionized further off axis and experience a larger radial ponderomotive force from the laser which leads to larger beam divergences.

Experiments were also performed at similar densities and comparable laser powers using pure helium. Weak electron spectra were occasionally observed over the range of P/P_c from 2 to 4 but the energy, divergence and energy spread of the spectra had large variations and were irreproducible. Simulations indicate that for our experimental parameters, the spectra produced from pure helium plasmas originate from electrons that are trapped into the 2nd and 3rd periods of the wakefield.

To understand how the injection of tunnel-ionized electrons into the wake reduces the necessary wake potential and therefore the a_o for trapping, we start from $\frac{d}{dt}(\gamma mc - P_z) = \frac{q}{c}\vec{V} \cdot \vec{E} - F_z$ which for electrons gives,

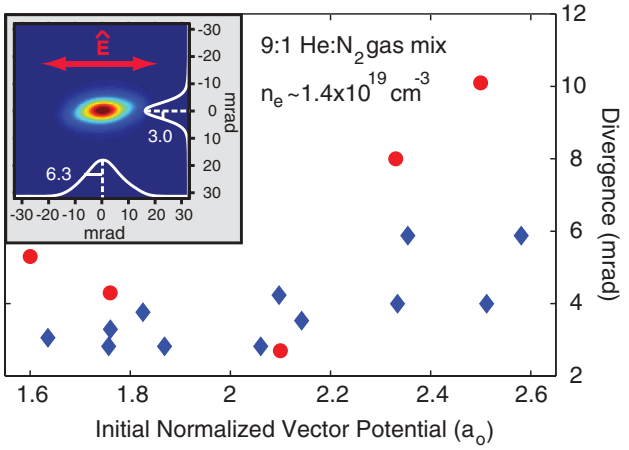

FIG. 5 (color online). Measured (diamonds) and simulated (circles) electron beam divergence ($e^{-1/2}$) transverse to the laser polarization vs laser a_o. An undispersed electron beam ($a_o \approx 2.1$) is shown inset, here the arrow indicates direction of laser polarization.

$$\frac{d}{d\xi}\frac{\bar{H}}{c} = \frac{-e}{1-\frac{v_z}{v_\phi}}\left[-\frac{\partial}{\partial s}\Phi + \left(\frac{\partial}{\partial s}\vec{A}\right)\cdot\frac{\vec{v}}{c}\right], \tag{1}$$

where z is the direction of laser propagation and we transform to the coordinates $\xi \equiv v_\phi t - z$, $s = z$, here $\bar{H} = \gamma mc^2 - v_\phi P_z - e(\Phi - \frac{v_\phi}{c}A_z)$, Φ and A_z are the components of the scalar and vector potential of the wake. For a particle beam driver $\frac{\partial}{\partial s} \to 0$, however the vector potential of a laser does not depend only on ξ since its phase velocity (and its group velocity) does not equal v_ϕ. For even a nonevolving laser field $\frac{\partial}{\partial s} \propto \frac{\omega_p^2}{\omega_o^2}$, therefore to the lowest order the right-hand side of Eq. (1) can be neglected. This leads to $\bar{H} = \text{const} = C_1$ for both laser and particle beam drivers. For an electron born at rest inside the wake (where $\Psi \neq 0$), it follows that

$$\gamma - \frac{v_\phi P_z}{mc^2} - \frac{e}{mc^2}\Psi = 1 - \frac{\Psi_i}{mc^2} \tag{2}$$

where the wake potential $\Psi \equiv \Phi - \frac{v_\phi}{c}A_z$ and $P_z = \gamma m v_z$. For a trapped electron ($v_z = v_\phi$) this gives,

$$\Delta\bar{\Psi} + 1 = \frac{\gamma}{\gamma_\phi^2} = \frac{\sqrt{1 + (P_\perp/mc)^2}}{\gamma_\phi}, \tag{3}$$

where $\Delta\bar{\Psi} = \frac{e}{mc^2}(\Psi_f - \Psi_i)$, $\gamma_\phi = (1 - (\frac{v_\phi}{c})^2)^{-1/2}$. The electron momentum perpendicular to the $\hat{z}$ direction, $P_\perp$, includes contributions from the vector potential at ionization, the ponderomotive force, and the transverse wakefield. Here subscripts i and f denote the initial injection and final trapping position, respectively. In the present work $P_\perp \lesssim mc^2$ and $\gamma_\phi \sim 10$ giving the trapping condition as $\Delta\bar{\Psi} \lesssim -1$.

Electrons born at the peak of the wake potential ($E_z = 0$) will experience the largest $|\Delta\bar{\Psi}_{\max}|$. If $\Delta\bar{\Psi}_{\max} < -1$ then electrons ionized earlier in the wake can also be trapped. In Fig. 1, electron 1 born close to the axis at ξ_{i1} experiences at $\Delta\bar{\Psi} \approx -1.2$, whereas electron 2, born earlier and off axis at ξ_{i2} experiences a $\Delta\bar{\Psi}(\xi, r) > -1$. Although both electrons are focused to ξ_f, only electron 1 satisfies the trapping condition. Electrons that form the wake are born near ξ_{i3}, and here do not experience a sufficient potential to become trapped. The maximum wake potential produced in the matched blowout regime (valid for $a_o \geq 2$) can be approximated as $\bar{\Psi}_{\max} \approx \frac{(k_p r_b)^2}{4} \approx a_o$, where r_b is the blowout radius and $k_p = \omega_p/c$ [11]. An a_o of 2 creates a $\Delta\bar{\Psi}_{\max} = -2$, which is sufficient to trap electrons. Results and simulations presented here show that an $a_o \sim 1.65$ is in fact sufficient to ionize and inject the 6th electron of nitrogen and create an adequate wake potential to trap it, whereas an $a_o \gtrsim 4$ is required to self-trap electrons in a preformed plasma [14].

In conclusion, experimental evidence for the tunneling ionization injection and subsequent trapping of electrons into laser-produced wakefields is presented. The spectral shape, relative amount of charge and beam divergence measured are in good agreement with the simulations. In comparison to self-trapping, tunneling ionization injection was shown to require a lower laser intensity to trap electrons, and could be a useful mechanism for injecting electrons into lower density wakefields.

Work supported by DOE grant DEFG02-92ER40727, NSF grant PHY-0936266 and FCT, Portugal (SFRH/BD/35749/2007). The authors would like to thank Chris Clayton of UCLA.

[1] W. P. Leemans *et al.*, Nature Phys. **2**, 696 (2006).
[2] E. Esarey *et al.*, Phys. Rev. Lett. **79**, 2682 (1997).
[3] J. Faure *et al.*, Nature (London) **444**, 737 (2006).
[4] C. G. R. Geddes *et al.*, Phys. Rev. Lett. **100**, 215004 (2008).
[5] D. Umstadter *et al.*, Phys. Rev. Lett. **76**, 2073 (1996).
[6] C. I. Moore *et al.*, Phys. Rev. Lett. **82**, 1688 (1999).
[7] E. Oz *et al.*, Phys. Rev. Lett. **98**, 084801 (2007).
[8] T. P. Rowlands-Rees *et al.*, Phys. Rev. Lett. **100**, 105005 (2008).
[9] R. A. Fonseca *et al.*, in *Lecture Notes in Computer Science 2329* (Springer, Heildberg, 2002), p. III–342.
[10] M. V. Ammosov, N. B. Delone, and V. P. Krainov, Sov. Phys. JETP **64**, 1191 (1986).
[11] W. Lu *et al.*, Phys. Rev. ST Accel. Beams **10**, 061301 (2007).
[12] G.-Z. Sun *et al.*, Phys. Fluids **30**, 526 (1987).
[13] J. E. Ralph *et al.*, Phys. Rev. Lett. **102**, 175003 (2009).
[14] F. S. Tsung *et al.*, Phys. Rev. Lett. **93**, 185002 (2004).
[15] S. P. D. Mangles *et al.*, IEEE Trans. Plasma Sci. **36**, 1715 (2008).
[16] E. Esarey *et al.*, Phys. Rev. A **42**, 3526 (1990).
[17] B. M. Penetrante *et al.*, J. Opt. Soc. Am. B **9**, 2032 (1992).
[18] Y. Glinec *et al.*, Europhys. Lett. **81**, 64001 (2008).
[19] S. P. D. Mangles *et al.*, Phys. Rev. Lett. **96**, 215001 (2006).